

Supporting Information:

Interfacial Self-Assembly of Graphene Networks at 1 vol% Enables Piezoresistive and Electrothermal Silicone Foams

Brenden Ferland¹ and Douglas Adamson^{1,2,*}

¹Polymer Program, Institute of Materials Science, University of Connecticut, Storrs, CT 06269; ²Department of Chemistry, University of Connecticut, Storrs, CT 06269

Contents

Table S1. Formulation Compositions for Graphene-Silicone PolyHIPE Foams

Figure S1. Four-Point (Kelvin) Probe Configuration

Figure S2. Sphere Size Distribution Analysis

Figure S3. Additional SEM Micrographs

Figure S4. Silica Accumulation at Oil-Water Interface

Figure S5. Effect of Crosslink Density on Mechanical Properties

Figure S6. Piezoresistive Response Under Cyclic Compression

Figure S7. Thermal Imaging of Electrothermal Heating

Figure S8. Temperature-Dependent Resistance

Table S1. Formulation Compositions for Graphene-Silicone PolyHIPE Foams**A. Percolation Series (Figure 2A)**

DMS-V21 (g)	HMS-301 (g)	Graphite (g)	Heptane (g)	DI Water (g)	Vol%	Conductivity (S/m)
44.50	5.35	0.85	5.06	61.39	0.36	Insulating
44.61	5.42	1.67	5.08	61.60	0.66	Insulating
47.38	5.36	2.37	5.17	61.15	1.04	0.003 ± 0.001
44.64	5.35	3.25	8.08	60.83	1.37	0.43 ± 0.04
44.78	5.35	6.94	5.02	63.51	2.22	0.86 ± 0.05
44.40	5.53	15.75	15.14	60.45	4.66	5.60 ± 0.99

B. Electrothermal Series (Figure 3)

Application	DMS-V21 (g)	DMS-H03 (g)	HMS-301 (g)	Graphite (g)	Heptane (g)	DI Water (g)	Vol%
Steady-state heating (Fig. 3A,B,D)	6.95	0.20	0.87	0.68	2.02	8.07	1.43
De-icing transient (Fig. 3C)	46.00	—	5.35	6.86	22.62	103.29	2.17

C. Crosslink Density Series (Figures S5, S6)

DMS-V21 (g)	DMS-H03 (g)	HMS-301 (g)	Graphite (g)	Heptane (g)	DI Water (g)	ρ_x (mmol/g)	Modulus (MPa)
4.65	—	0.54	0.39	0.51	7.11	0.314	0.515
4.94	0.09	0.53	0.38	0.51	7.26	0.311	0.390
4.92	0.14	0.55	0.38	0.50	7.17	0.307	0.348
4.83	0.19	0.57	0.39	0.50	7.04	0.302	0.280
4.75	0.24	0.54	0.39	0.51	7.44	0.301	0.269
4.75	0.37	0.55	0.39	0.52	7.30	0.293	0.169

Crosslink density (ρ_x) calculated as mmol vinyl per gram silicone based on DMS-V21 vinyl functionality: $\rho_x = (\text{mass}_{\text{DMS-V21}} \times 0.35 \text{ mmol/g}) / (\text{mass}_{\text{DMS-V21}} + \text{mass}_{\text{HMS-301}} + \text{mass}_{\text{DMS-H03}})$. All formulations used Nano 24 natural flake graphite (median flake size $\approx 1 \mu\text{m}$) from Asbury Carbons. Volume percentages calculated using foam densities and graphite density of 2.26 g/cm^3 . “—” indicates component not used in formulation. All masses are actual measured values.

Four-Point (Kelvin) Probe Configuration

Through-Thickness Conductivity Measurement

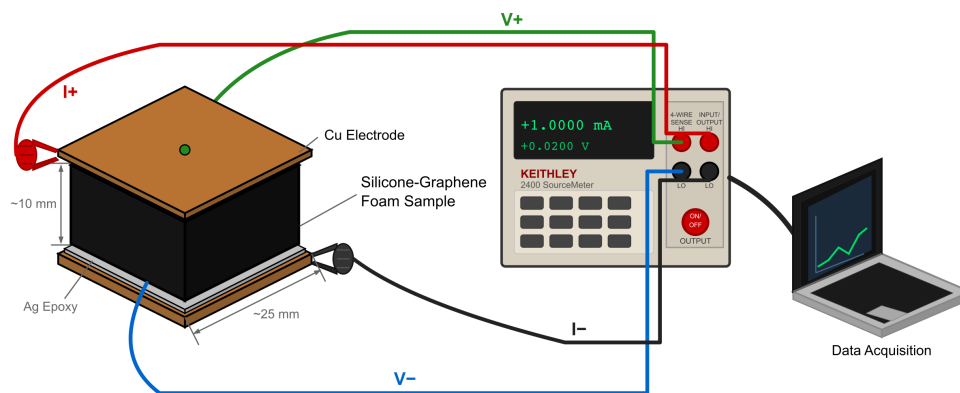


Figure S1. Four-point (Kelvin) probe configuration for through-thickness conductivity measurement. Silicone-graphene foam specimens (approximately $25 \times 25 \times 10 \text{ mm}$) were contacted with copper foil electrodes adhered to opposing faces using silver conductive epoxy (MG Chemicals 8331D). Current (I^+ , I^-) was sourced through the electrodes while voltage (V^+ , V^-) was measured separately via alligator clips attached directly to the copper foil. A Keithley 2400 source measure unit provided test current with simultaneous voltage acquisition.

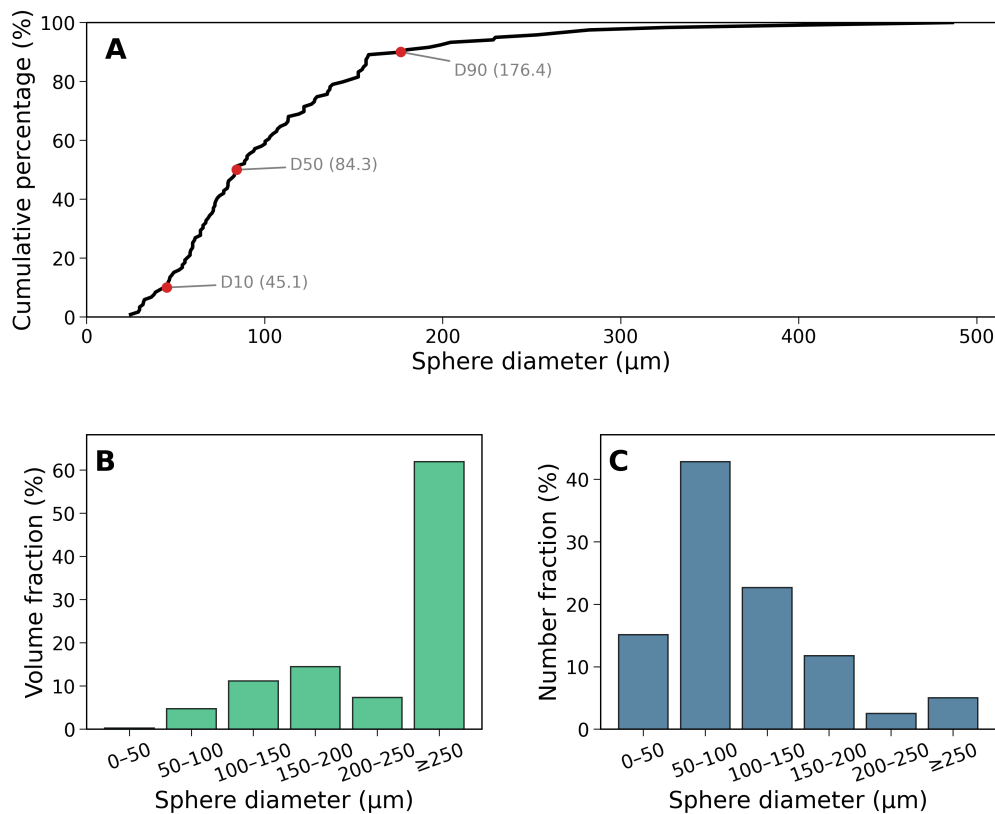


Figure S2. Sphere size distribution analysis of graphene-stabilized silicone polyHIPE foams. (A) Cumulative distribution function showing $D_{10} = 45.1 \mu\text{m}$, $D_{50} = 84.3 \mu\text{m}$, and $D_{90} = 176.4 \mu\text{m}$. (B) Volume fraction distribution with largest contribution from $\geq 250 \mu\text{m}$ spheres (62%). (C) Number fraction distribution with peak frequency in 50–100 μm range (42.9%). Analysis based on $n = 119$ spheres from SEM imaging of two independent samples.

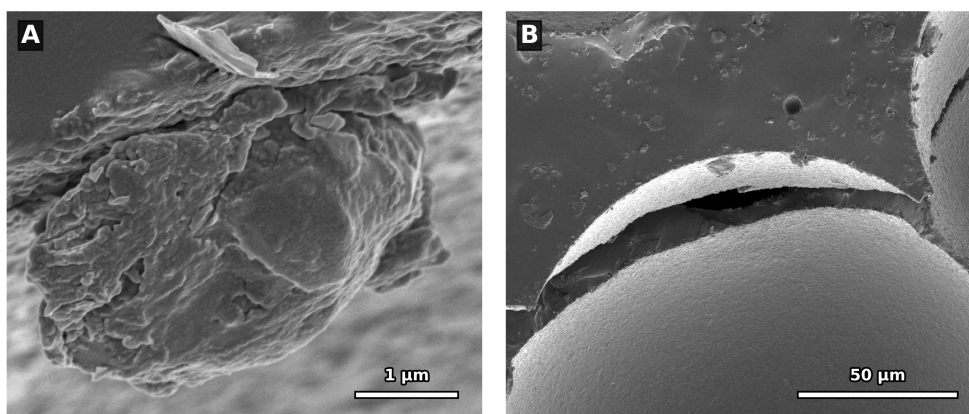


Figure S3. Scanning electron micrographs providing additional detail on graphene distribution and cell wall architecture in silicone-graphene polyHIPE foams. (A) High-magnification image showing graphene and graphite flakes self-assembled at the cell surface, demonstrating that both few-layer graphene sheets and larger graphite particles localize at the oil-water interface during emulsion templating (scale bar: $1 \mu\text{m}$). (B) Lower-magnification view of a cell wall revealing the layered internal structure, with the graphene-rich region visible as a distinct layer within the silicone matrix (scale bar: $50 \mu\text{m}$).



Figure S4. Competitive adsorption of hydrophobic silica at the oil-water interface. Photograph of a graphene-silicone interface prepared with HMDZ-modified fumed silica, showing accumulation of hydrophobic silica particles (light band) at the silicone-water interface.

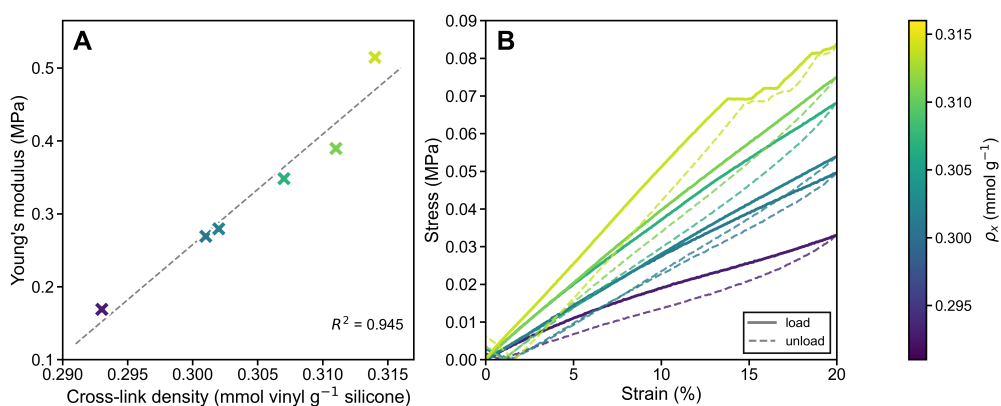


Figure S5. Effect of crosslink density on mechanical properties of graphene-silicone polyHIPE foams. (A) Young's modulus as a function of crosslink density (ρ_x), expressed as mmol vinyl per gram silicone. Dashed line indicates linear regression ($R^2 = 0.945$). (B) Representative stress-strain curves during cyclic compression to 20% strain for samples spanning the crosslink density range. Solid lines indicate loading; dashed lines indicate unloading. Color scale corresponds to crosslink density.

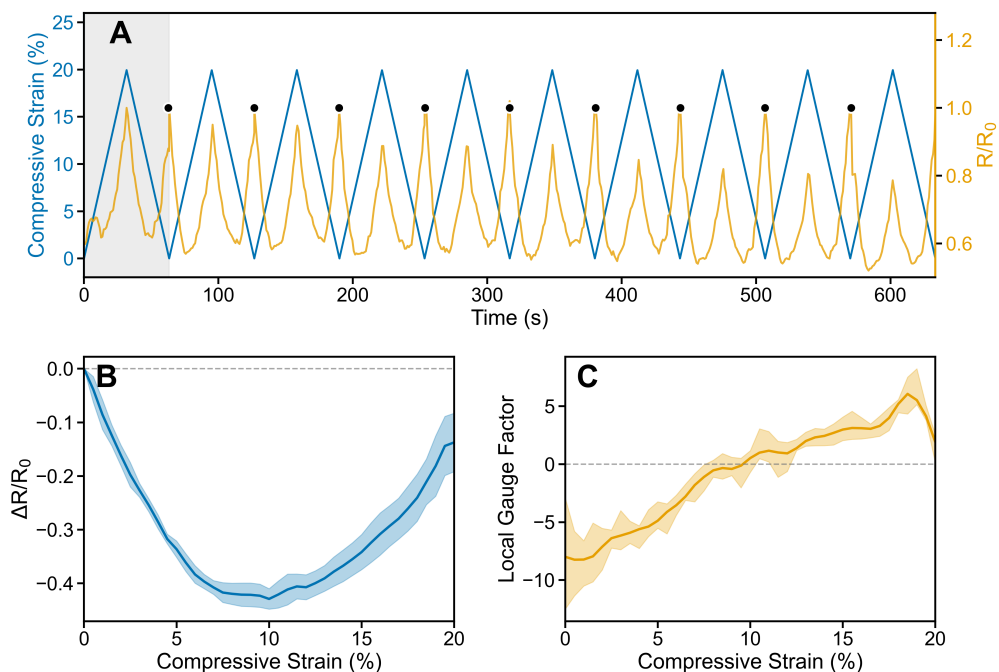


Figure S6. Piezoresistive response of silicone-graphene polyHIPE foam under cyclic compression. (A) Time series showing compressive strain (blue, left axis) and normalized resistance R/R_0 (orange, right axis) during 20% cyclic loading. Black circles indicate R_0 measurement points. Gray shading denotes the first partial cycle excluded from analysis due to non-equilibrium conditioning effects. (B) Normalized resistance change $\Delta R/R_0$ versus compressive strain, showing a U-shaped response with minimum ($\Delta R/R_0 = -0.43 \pm 0.01$) at the inflection point of $9.3 \pm 1.0\%$ strain. (C) Local gauge factor ($d(\Delta R/R_0)/d\epsilon$) versus strain, transitioning from negative (resistance decreasing) to positive (resistance increasing) at the inflection point. Solid lines represent means across 8 complete cycles; shaded regions indicate ± 1 standard deviation.

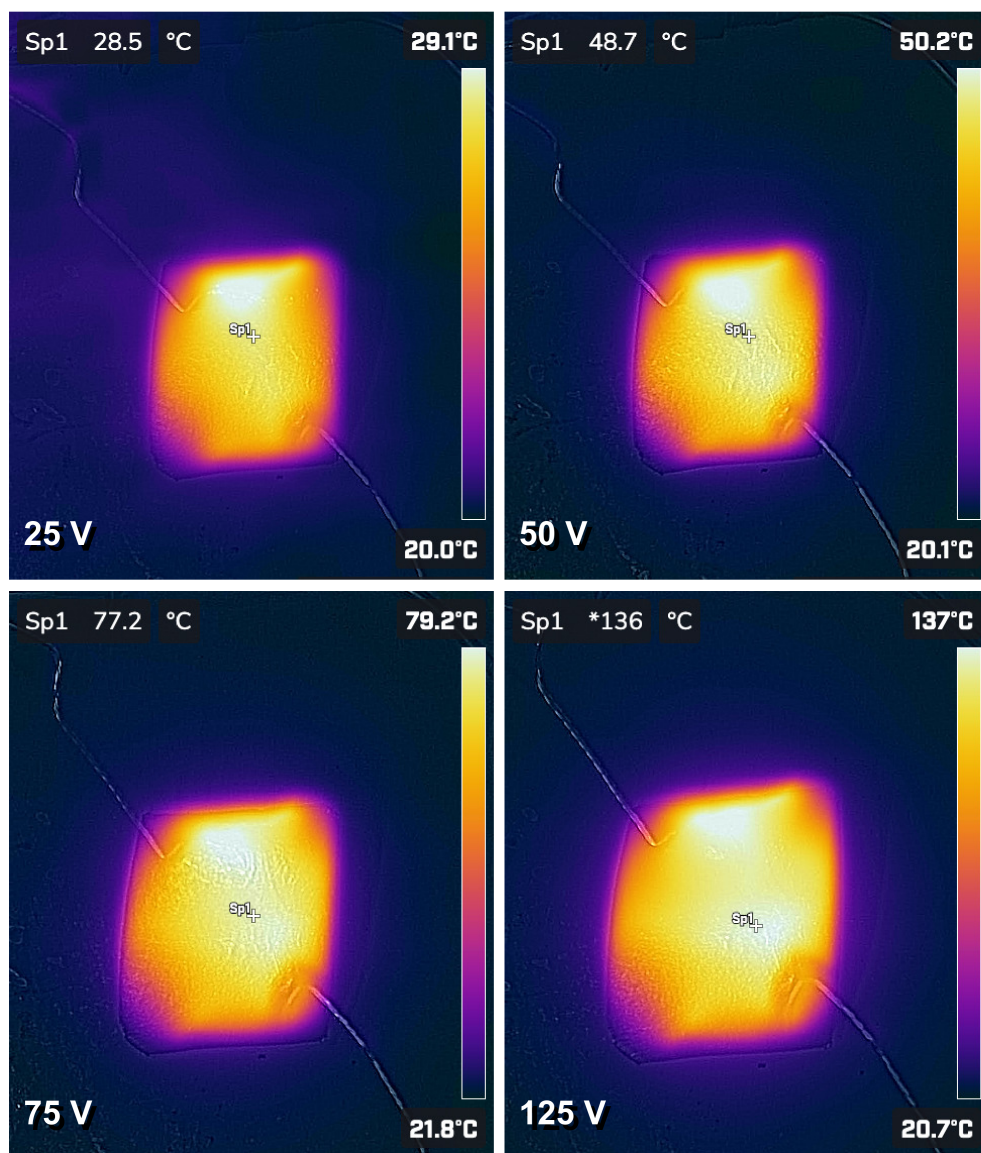


Figure S7. Infrared thermal imaging of electrothermal heating in graphene-silicone foam (1.43 vol% graphene loading). Steady-state surface temperature distributions are shown at applied voltages of 25 V (28.5 °C), 50 V (48.7 °C), 75 V (77.2 °C), and 125 V (136 °C). Temperature values indicate point measurements.

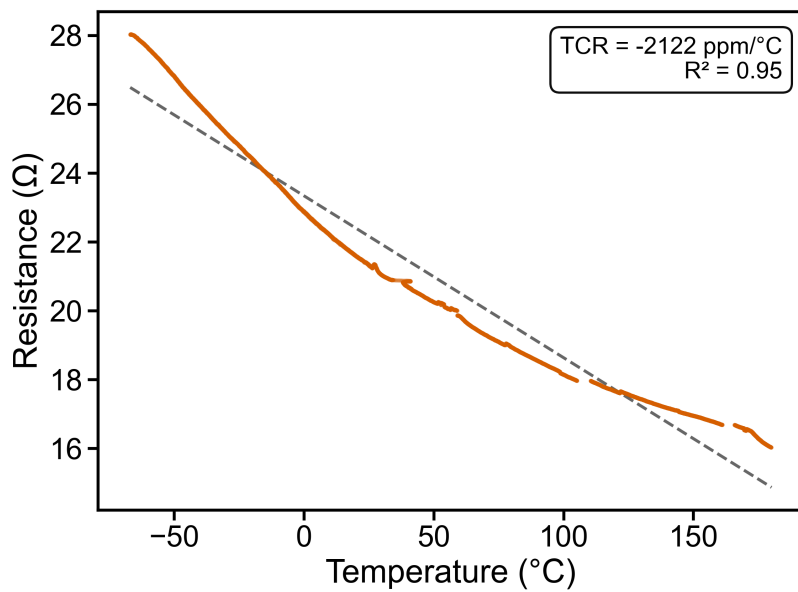


Figure S8. Temperature-dependent resistance of silicone-graphene polyHIPE foam from $-67\text{ }^{\circ}\text{C}$ to $180\text{ }^{\circ}\text{C}$. Dashed line indicates linear fit ($\text{TCR} = -2122\text{ ppm}/^{\circ}\text{C}$, $R^2 = 0.95$).